

# Chirality control of a Cu(I)·(phenanthroline)<sub>2</sub> complex by a sugar–boronic acid interaction. A preliminary step toward the total chain helicity control by a chain-end sugar-binding

2 PERKIN

Masashi Yamamoto,<sup>a</sup> Masayuki Takeuchi,<sup>a</sup> Seiji Shinkai,<sup>\*a</sup> Fumito Tani<sup>b</sup> and Yoshinori Naruta<sup>b</sup>

<sup>a</sup> Department of Chemistry & Biochemistry, Graduate School of Engineering, Kyushu University, Hakozaki, Fukuoka 812-8581, Japan

<sup>b</sup> Institute for Fundamental Research of Organic Chemistry, Kyushu University, Hakozaki, Fukuoka 812-8581, Japan

Received (in Cambridge, UK) 21st June 1999, Accepted 1st November 1999

Compounds **1a** and **1b** which have a 1,10-phenanthroline moiety, were synthesized in order to form a helical structure in the presence of Cu(I), and a boronic acid moiety with which to bind a saccharide at the chain end. When saccharides were added, the Cu(I) complexes (as **1a**<sub>2</sub>·Cu(I) and **1b**<sub>2</sub>·Cu(I)) gave the CD-active species reflecting the absolute configurational structure of saccharides. Thus, the P versus M helicity of the complexes can be controlled by the boronic acid–saccharide interaction. The results show that the terminal boronic acid group is useful to create the chiral helical structure and the total helicity is governed by the chirality of the boronic acid-bound saccharide.

## Introduction

Helical complexes have been of great interest as examples of self-assembled supramolecular structures in artificial systems and as models for DNA and RNA structures in nature.<sup>1</sup> One important characteristic which differentiates the helical structure from other supramolecular structures is the ‘chirality’ generated by the twisting direction along the one-dimensional chain.<sup>2–15</sup> In general, the ‘chirality’ is created by the introduction of chiral substituents into ‘helicates’. Meanwhile, Hamilton *et al.*<sup>16</sup> have demonstrated that self-assembled helical metal complexes with terminal hydrogen-bonding sites are useful for the recognition of dicarboxylic acid guests. The results imply that the host–guest-type interaction at the helical chain end may crucially control the twisting direction of the total chain helicity. Recently, it has been shown that boronic acid–saccharide covalent interactions, which form readily and reversibly in aqueous media, represent an important alternative binding force for the recognition of saccharides and related molecular species.<sup>17–30</sup> Here, it occurred to us that the chirality of the helical metal complexes created from helicates bearing a terminal boronic acid group may be reversibly controlled by the boronic acid–saccharide interaction. If this working hypothesis is correct, it follows that a saccharide library, containing abundant chirality resources, would be useful to create a variety of helical structures. As the first step to test this intriguing working hypothesis, we designed compounds **1a** and **1b** which have a 1,10-phenanthroline moiety with which to constitute the helical metal complex and an *o*-aminomethylphenyl boronic acid moiety with which to bind saccharides at the helical chain end. Compound **1a** was mainly used for the absorption and CD spectroscopic studies whereas compound **1b** was used for the <sup>1</sup>H NMR spectroscopic studies because the *p*-anisyl group gives well-split peaks which are useful as a marker to detect configurational changes. Interestingly, we have found that, as shown in Scheme 1, added saccharides can influence the equilibrium between plus (P) and minus (M) enantiomers, reflecting their absolute configurational structure.<sup>31</sup>

## Results and discussion

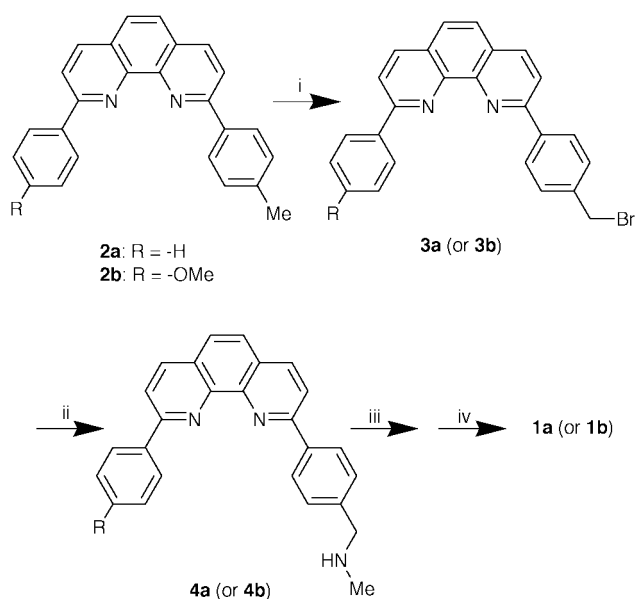
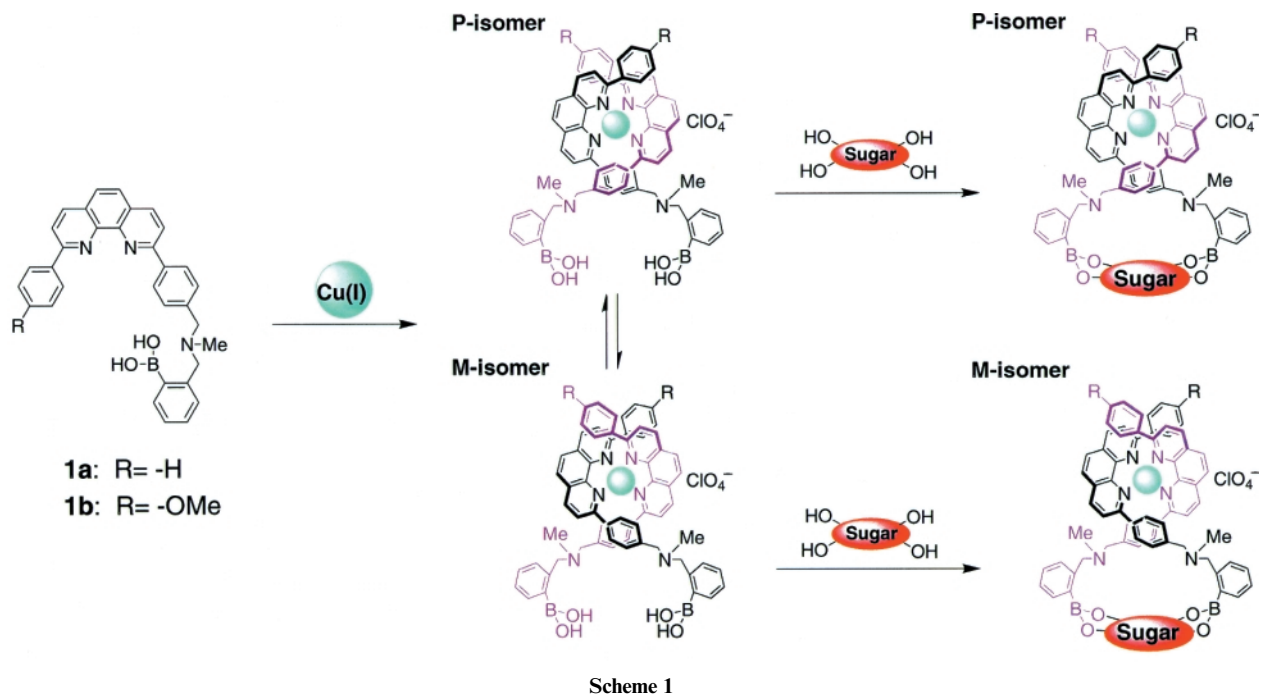
### Molecular design and synthesis of ligands (**1a** and **1b**)

To test the working hypothesis we chose the chiral induction in a Cu(I)·(1,10-phenanthroline) complex. Examination with CPK molecular models and computational tools suggested that introduction of a boronic acid group into the 9-position of 1,10-phenanthroline *via* a phenyl group would satisfy the requirements: that is, the metal-binding 1,10-phenanthroline site is moderately insulated by the phenyl group from the saccharide-binding boronic acid site whereas the chirality in the Cu(I) complex seems sterically controllable by the boronic acid–saccharide interaction. The *o*-aminomethyl group interacts intramolecularly with the boronic acid group and stabilises the saccharide complex.<sup>9,10</sup> Thus, compounds **1a** (mp 174–179 °C) and **1b** (mp 179–183 °C) were synthesised from 2-phenyl-9-*p*-tolyl-1,10-phenanthroline (**2a**) and 2-*p*-anisyl-9-*p*-tolyl-1,10-phenanthroline (**2b**), respectively, according to Scheme 2 and identified by <sup>1</sup>H NMR and IR spectral evidence and elemental analyses (see Experimental section).

### Absorption spectra of the Cu(I) complexes

The spectral patterns of both absorption and fluorescence spectroscopies changed with the concentration of **1a** in 100% aqueous solution. This implies that **1a** tends to aggregate in 100% aqueous solution. To avoid this complexity, the spectroscopic measurements were carried out in MeOH–MeCN = 1 : 1 (v/v) at 25 °C. In this medium both absorption and fluorescence intensities showed a linear relationship with respect to the concentration of **1a**.

Fig. 1 shows the absorption spectral change induced by the Cu(I) addition (added as [Cu(MeCN)<sub>4</sub>]ClO<sub>4</sub>). The λ<sub>max</sub> at 309 nm decreased while that at 439 nm increased (as shown in an inserted figure) with tight isosbestic points at 364 and 292 nm. The plots of the absorbances against [Cu(I)]/[**1a**] (Fig. 2) afforded a clear break-point at 0.5, indicating that the complex consists of one Cu(I) and two **1a** ligands (as illustrated in Scheme 1). In the subsequent CD measurements we enhanced



**Scheme 2** Reagents and conditions (yield): i, NBS, AIBN,  $\text{CCl}_4$ , reflux; ii,  $\text{MeNH}_2$ ,  $\text{CCl}_4$  (62%, calculated from **2a** or 46%, calculated from **2b**); iii,  $\text{K}_2\text{CO}_3$ , MeCN, reflux; iv,  $\text{H}_2\text{O}$  (46%, calculated from **4a** or 34%, calculated from **4b**).

the concentrations up to  $[\mathbf{1a}] = 0.200 \text{ mmol dm}^{-3}$  and  $[\text{Cu(I)}] = 0.100 \text{ mmol dm}^{-3}$  because the CD spectral change was not so sensitive as the absorption spectral change. Judging from the sharp break-point in Fig. 2, one can assume that **1a** and Cu(I) are fully converted to the  $\mathbf{1a}_2\cdot\text{Cu(I)}$  complex under these CD measurement conditions.

#### Stoichiometry of the $\mathbf{1a}_2\cdot\text{Cu(I)}\cdot\text{D-glucose}$ complex

In order to estimate the chiral twisting ability of monosaccharides for the  $\mathbf{1a}_2\cdot\text{Cu(I)}$  complex we primarily tested D-glucose as a representative monosaccharide. When D-glucose was added to the  $\mathbf{1a}_2\cdot\text{Cu(I)}$  complex solution, the CD bands appeared gradually at 250–350 nm region and 400–600 nm region (MLCT region: Fig. 3). This slow CD appearance implies that D-glucose is bound to the boronic acid groups rather slowly in the organic medium and/or D-glucose-induced conversion of one enantiomer to other occurs slowly. The appearance of the CD bands

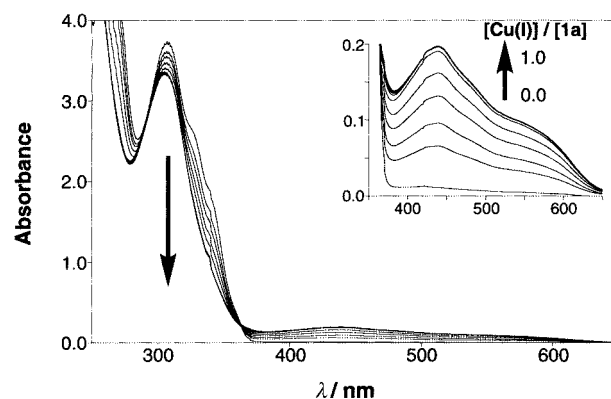


**Fig. 1** Absorption spectral change of **1a** ( $0.100 \text{ mmol dm}^{-3}$ ) with increasing Cu(I) concentration.

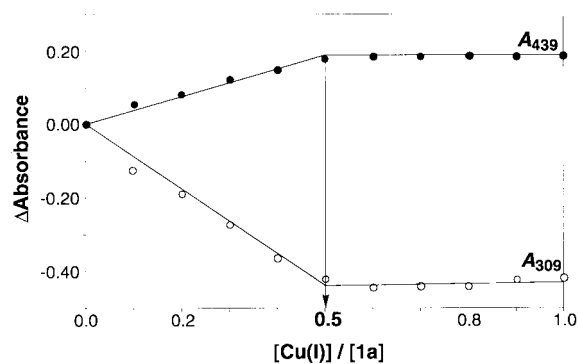


**Fig. 2** Plots of absorbance versus  $[\text{Cu(I)}]/[\mathbf{1a}]$ : ●, 439.0 nm, ○, 309.0 nm.

means that one enantiomer of the ternary complex has become in excess of the other. A plot of the CD intensity vs. time revealed that the CD intensity becomes constant after 6–7 h. In the following experiments, therefore, we measured the final CD spectra after 12 h. The continuous variation plots of the CD intensity vs.  $[\mathbf{1a}_2\cdot\text{Cu(I)}]/([\mathbf{1a}_2\cdot\text{Cu(I)}] + [\text{D-glucose}])$  provided a maximum at 0.5, indicating that the ternary complex consists of 1:1 stoichiometric  $\mathbf{1a}_2\cdot\text{Cu(I)}$  and D-glucose (Fig. 4). This finding was also supported by mass spectrometry (ESI-MS). To a MeCN–MeOH = 1:1 (v/v) solution containing the  $\mathbf{1a}_2\cdot\text{Cu(I)}$

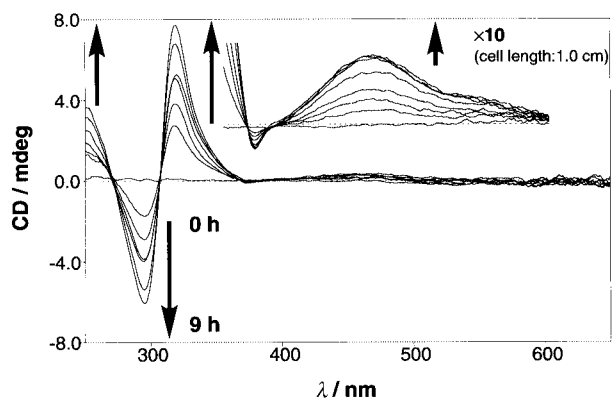


Fig. 3 Time dependence of the CD appearance after the addition of D-glucose ( $0.100 \text{ mmol dm}^{-3}$ ) to the solution containing  $\mathbf{1a}_2 \cdot \text{Cu(I)}$  ( $0.100 \text{ mmol dm}^{-3}$ ): cell length  $0.1 \text{ cm}$ ; (inserted) cell length  $1.0 \text{ cm}$ .

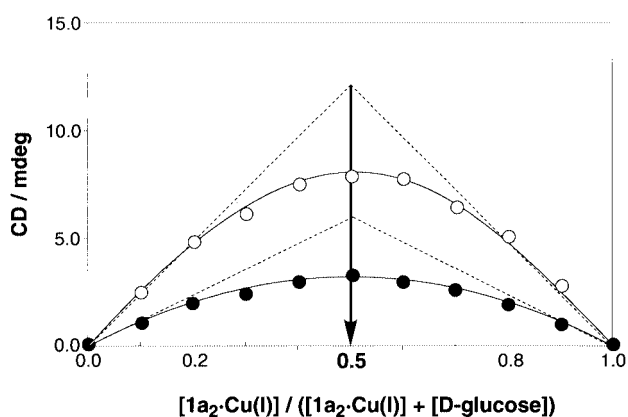


Fig. 4 Continuous variation plots: the  $[\mathbf{1a}_2 \cdot \text{Cu(I)}] + [\text{D-glucose}]$  concentration was maintained constant ( $0.200 \text{ mmol dm}^{-3}$ ): ●,  $463.0 \text{ nm}$ , ○,  $318.5 \text{ nm}$ .

complex ( $1.00 \times 10^{-4} \text{ mol dm}^{-3}$ ) was added D-glucose ( $5.00 \times 10^{-4}$  or  $7.50 \times 10^{-4} \text{ mol dm}^{-3}$ ) and the solution was incubated at  $25^\circ \text{C}$  for 12 h. This solution was subjected to the ESI-MS measurement. One strong peak ( $m/z = 1189$ ) and several weak accompanying peaks with  $\Delta m/z = 1.0$  were observed. The results indicate that the major species under the ESI-MS measurement conditions is  $[\mathbf{1a}_2 \cdot \text{Cu(I)} \cdot \text{D-glucose}]^+$ . These spectroscopic data consistently support the complexation mode as illustrated in Scheme 1: that is, the  $\mathbf{1}_2 \cdot \text{Cu(I)}$  complex binds one D-glucose molecule with two boronic acid–diol interactions to form a macrocyclic structure.

#### Possible correlation between the saccharide structure and the CD sign

The CD spectra were measured as a function of the D- and L-glucose concentrations while the concentration of  $\mathbf{1a}_2 \cdot \text{Cu(I)}$  was maintained constant ( $1.00 \times 10^{-4} \text{ mol dm}^{-3}$ ). The CD spectra changed with a few tight isosbestic points. As expected, the CD spectra obtained in the presence of L-glucose were symmetrical to those obtained in the presence of D-glucose (Fig. 5). Plots of the CD intensities at 319 and 464 nm vs. the D- and L-glucose concentrations are shown in Fig. 6. From analysis of the plots in Fig. 6 by computational curve fitting one can estimate the binding constant ( $K_b$ ) to be  $4800 \pm 400 \text{ dm}^3 \text{ mol}^{-1}$  for both D- and L-glucose.<sup>32</sup>

Fig. 5 indicates that at the MLCT region (400–600 nm) D-glucose gives the positive CD sign whereas L-glucose gives the negative CD sign. The past CD studies on chiral bipyridine-based helicate–Cu(I) complexes have established that the positive CD sign is generated from the P-isomer whereas the negative CD sign is generated from the M-isomer:<sup>6,7,9</sup> that is, D-glucose twists the  $\mathbf{1a}_2 \cdot \text{Cu(I)}$  complex into the P chirality

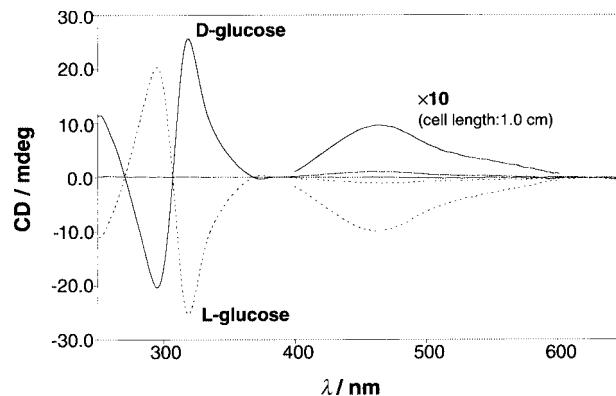


Fig. 5 CD spectra of  $\mathbf{1a}_2 \cdot \text{Cu(I)}$  ( $0.100 \text{ mmol dm}^{-3}$ ) in the presence of D- or L-glucose ( $7.50 \text{ mmol dm}^{-3}$ ).

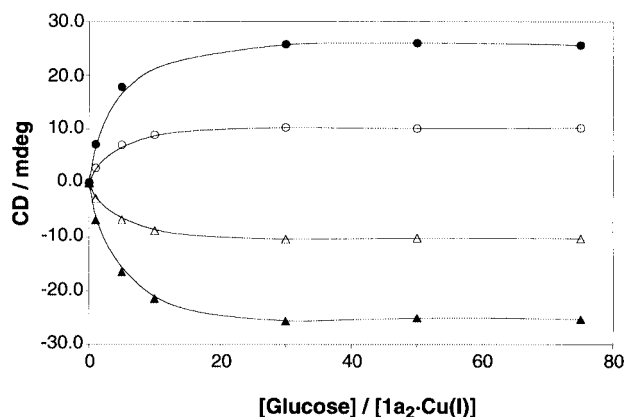


Fig. 6 Plots of CD intensities (319 and 464 nm) vs. D- and L-glucose concentrations:  $[\mathbf{1a}_2 \cdot \text{Cu(I)}] = 0.100 \text{ mmol dm}^{-3}$ , D-glucose (●,  $319 \text{ nm}$ , ○,  $464 \text{ nm}$ ), L-glucose (▲,  $319 \text{ nm}$ , △,  $464 \text{ nm}$ ).

motif (clockwise direction around the central axis connecting Cu(I) with glucose) whereas L-glucose twists it into the M chirality motif (anti-clockwise direction around the central axis connecting Cu(I) with glucose). The exciton-coupling CD bands at around 300 nm reflect the  $\pi\text{-}\pi^*$  transition in the phenanthroline moieties. Examination of the CD sign reveals that the positive exciton-coupling interaction is observed for D-glucose whereas the negative exciton-coupling interaction is observed for L-glucose (Fig. 5): that is, P-isomer and M-isomer in the MLCT region are always correlated with the positive exciton-coupling interaction and the negative exciton-coupling interaction, respectively, in the phenanthroline moieties.

To obtain a possible correlation between the saccharide structure and the CD sign we measured the CD spectra of  $\mathbf{1a}_2 \cdot \text{Cu(I)}$  for seven D-saccharides in addition to D-glucose. The structures are illustrated in Scheme 3 (mainly, as their pyranose forms).

Firstly, we compared the CD spectra of D-mannose, D-allose and D-galactose which are classified into epimers of D-glucose. The typical concentration-dependent CD spectra and the typical plots of the CD intensity at the exciton-coupling band versus [D-saccharide] are shown in Figs. 7 and 8. Examination of these figures, together with that of Figs. 5 and 6, reveals that (i) D-mannose and D-galactose give the positive CD sign for the MLCT region and the positive exciton-coupling band for the phenanthroline region like D-glucose whereas D-allose gives the negative CD sign for the MLCT region and the negative exciton-coupling band for the phenanthroline region like L-glucose, (ii) the plus–minus in the MLCT region is always correlated with the plus–minus in the phenanthroline  $\pi\text{-}\pi^*$  transition region and (iii) the absolute CD intensities in the MLCT region and the phenanthroline region both appear in the order of D-glucose > D-galactose > D-mannose > D-allose.

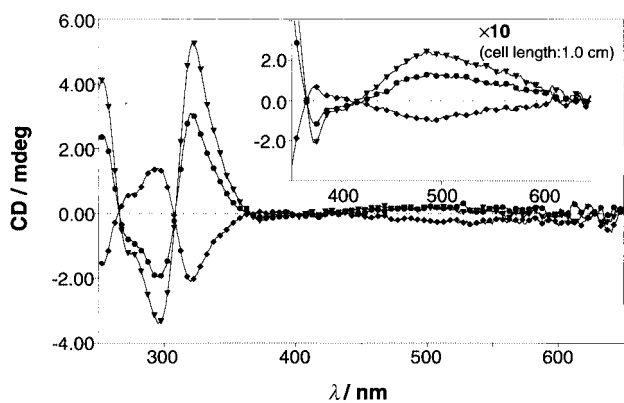
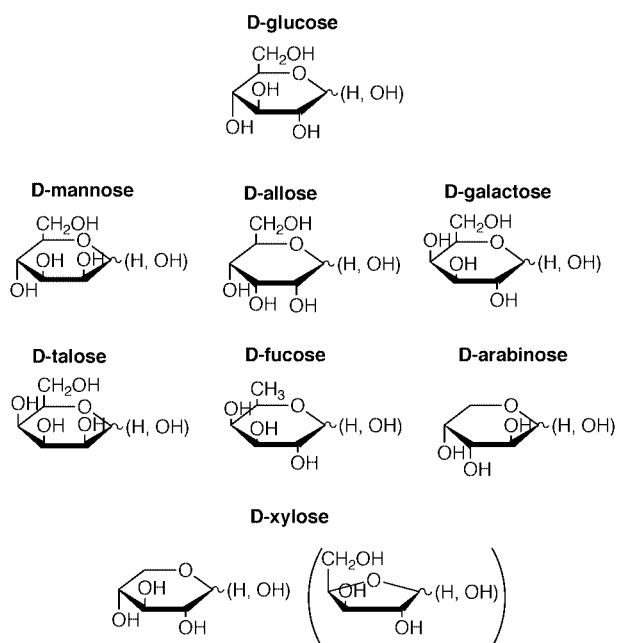


Fig. 7 CD spectra of  $1a_2 \cdot Cu(I)$  ( $0.100 \text{ mmol dm}^{-3}$ ) in the presence of saccharide;  $\nabla$ ; D-fucose ( $7.50 \text{ mmol dm}^{-3}$ ),  $\bullet$ ; D-galactose ( $1.50 \text{ mmol dm}^{-3}$ ),  $\blacklozenge$ ; D-mannose ( $3.00 \text{ mmol dm}^{-3}$ ).



Scheme 3

Most interesting is the finding that the CD signs for D-allose are inverted from those for other three saccharides.

The spectroscopic data are summarised in Table 1. Eight saccharides tested herein all afforded the CD-active species with  $1a_2 \cdot Cu(I)$  and the plus-minus in the MLCT region is correlated with the plus-minus in the phenanthroline  $\pi-\pi^*$  transition region (except D-talose, which did not give a clear exciton-coupling band). Very interestingly, we noticed that the plus-minus in the MLCT region is predictable from the absolute configuration of the 3-OH: when the 3-OH group is 'up', the MLCT region becomes plus whereas when it is 'down', the MLCT region becomes minus. The origin of this intriguing correlation is not yet explicable. We now consider that when the 1,2-diol group forms a complex with the boronic acid group,<sup>21,22</sup> the absolute configuration of the neighboring 3-OH affects the twisting direction of the  $1a_2 \cdot Cu(I)$ -saccharide complexes. On the other hand, 1-methyl- $\alpha$ -D-glucopyranoside, in which the 1-OH group useful for the complexation is protected by the methyl group, was CD-silent. This suggests an idea that as already reported in related system,<sup>21,22,25</sup> the 1,2-diol in monosaccharides acts as an essential boronic acid-binding site.

As a summary of the foregoing findings, one can now regard that the chirality in D-saccharides is transmitted to the helicity in the metal complex.

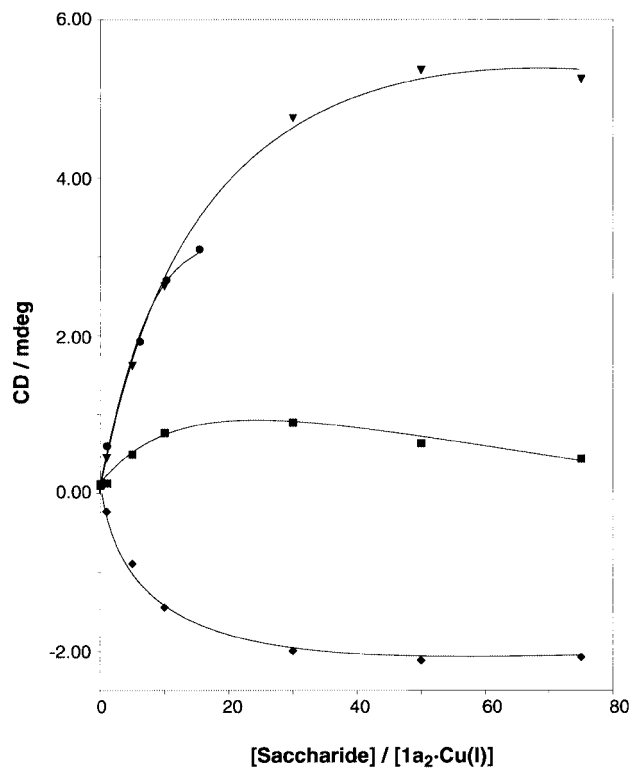


Fig. 8 Plots of the CD intensity vs. [saccharide]:  $\nabla$ ; D-fucose,  $\bullet$ ; D-galactose,  $\blacklozenge$ ; D-arabinose,  $\blacksquare$ ; D-mannose.

#### Estimation of the binding constants ( $K_b$ )

From plots of the CD intensity at the  $\pi-\pi^*$  transition band against [D-saccharide] (Fig. 8) the  $K_b$  values were estimated assuming the formation of  $1a_2 \cdot Cu(I)$ :D-saccharide = 1:1 complexes. The band for D-talose was too weak to estimate the  $K_b$  accurately. The plot for D-mannose was biphasic. It has been established through the CD spectroscopic studies that the complex becomes CD-active only when the saccharide is recognised by the host at least at two points, forming a 1:1 stoichiometric cyclic structure whereas it becomes CD-silent when it is converted into a 1:2 host/saccharide noncyclic structure in the high saccharide concentration region.<sup>22,23,25,33,34</sup> This plot suggests, therefore, a shift of a  $1a_2 \cdot Cu(I)$ :D-mannose = 1:1 cyclic complex to a  $1a_2 \cdot Cu(I)$ :D-saccharide = 1:2 noncyclic complex (CD-silent)<sup>25</sup> with increasing D-mannose concentration.<sup>22-25</sup> Hence, both the  $K_b$  for the 1:1 complex with seven saccharides and the  $K_b'$  for the 1:2 complex with D-mannose were estimated by analysing these plots with a non-linear least-squares method.<sup>32-34</sup> The results are summarised in Table 2.

It is seen from Table 2 that (i) the  $K_b$  values appear in the order of D-glucose > D-mannose > D-xylose > D-arabinose > D-galactose > D-fucose > D-allose, (ii) six D-saccharides (except D-mannose) show a single saturation curve, indicating that the cyclic  $1a_2 \cdot Cu(I)$ :D-mannose = 1:1 complex is more stable than the noncyclic  $1a_2 \cdot Cu(I)$ :D-saccharide = 1:2 complex and (iii) only in the binding of D-mannose, the formation of the noncyclic 1:2 complex can compete with that of the cyclic 1:1 complex although the  $K_b$  is still greater by 14-fold than the  $K_b'$ . The order of the  $K_b$  values is approximately coincident with the order of the CD intensity (D-glucose > D-galactose > D-mannose > D-allose: *vide supra*). This implies that the more stable is the cyclic 1:1 complex, the more stronger becomes the CD intensity. On the other hand, it is not clear yet why the  $K_b'$  for the D-mannose complex is exceptionally large compared with others in spite of the large  $K_b$  next to D-glucose.

Why does  $1a_2 \cdot Cu(I)$  generally tend to form P-isomers with D-monosaccharides (except D-arabinose and D-allose)? In the

**Table 1** CD spectroscopic data obtained in the presence of various monosaccharides<sup>a</sup>

| Monosaccharide                | $\pi$ - $\pi^*$ band <sup>b</sup>   |   | MLCT band <sup>c</sup> | Helicity | Structure of monosaccharide |      |
|-------------------------------|---|---|------------------------|----------|-----------------------------|------|
|                               | $\lambda_{\max}$ or $\lambda_{\min}$ /nm<br>(CD <sub>max</sub> or $\lambda_{\min}$<br>intensity/mdeg) | $\lambda_{\max}$ or $\lambda_{\min}$ /nm<br>(CD <sub>max</sub> or $\lambda_{\min}$<br>intensity/mdeg) |                        |          | 1,2-diol                    | 3-OH |
| D-Glucose                     | 319.0<br>(25.61)  | 295.0<br>(-20.34)   | 463.5<br>(10.23)       | P        | down                        | up   |
| D-Fucose                      | 322.0<br>(5.25)   | 299.5<br>(-3.38)  | 480.5<br>(2.31)        | P        | down                        | up   |
| D-Galactose                   | 321.5<br>(3.06)   | 290.0<br>(-1.97)  | 498.0<br>(1.38)        | P        | down                        | up   |
| D-Xylose                      | 318.0<br>(1.85)   | 297.5<br>(-0.51)  | 458.0<br>(0.64)        | P        | down                        | up   |
| D-Mannose                     | 319.0<br>(0.89)   | 296.0<br>(-0.86)  | 463.5<br>(0.50)        | P        | up                          | up   |
| D-Talose                      | 317.5<br>(1.01)   |   | 511.5<br>(0.56)        | P        | up                          | up   |
| D-Arabinose                   | 319.5<br>(-2.12)  | 295.0<br>(1.51)   | 490.5<br>(-1.03)       | M        | up                          | down |
| D-Allose                      | 319.5<br>(-1.00)  | 290.0<br>(0.56)   | 491.0<br>(-0.47)       | M        | down                        | down |
| Methyl- $\alpha$ -D-glucoside | CD silent   |   | CD silent              |          |                             |      |

<sup>a</sup> [**1a**<sub>2</sub>·Cu(I)] = 0.100 mmol dm<sup>-3</sup>, [monosaccharide] = 7.50 mmol dm<sup>-3</sup> ([D-galactose] = 1.50 mmol dm<sup>-3</sup> [D-mannose] = 3.00 mmol dm<sup>-3</sup>), MeOH–MeCN = 1 : 1 (v/v), 25 °C. <sup>b</sup> Cell length: 0.1 cm. <sup>c</sup> Cell length: 1.0 cm.

**Table 2** Association constants for saccharides with **1a**<sub>2</sub>·Cu(I)<sup>a</sup>

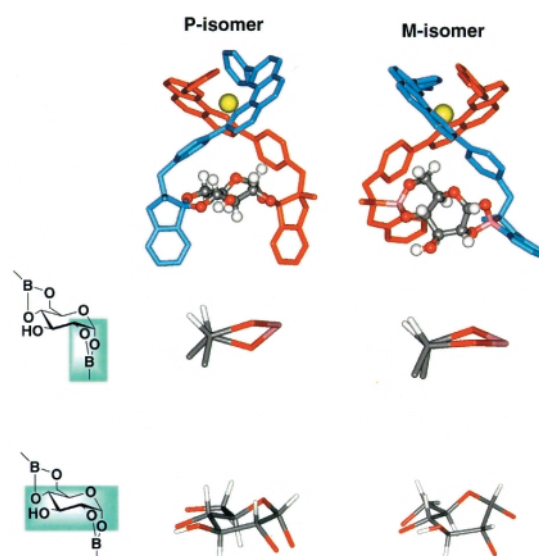
| Monosaccharide | $K_b$ /dm <sup>3</sup> mol <sup>-1</sup> | $K_b'$ /dm <sup>3</sup> mol <sup>-1</sup> |
|----------------|--|---|
| D-Glucose      | 4800 ± 400                               | —   |
| D-Fucose       | 760 ± 120                                | —   |
| D-Galactose    | 1300 ± 320                               | —   |
| D-Xylose       | 1700 ± 200                               | —   |
| D-Mannose      | 2100 ± 800                               | 150                                       |
| D-Talose       | —  | —   |
| D-Arabinose    | 1500 ± 200                               | —   |
| D-Allose       | 700 ± 100                                | —   |

<sup>a</sup> [**1a**<sub>2</sub>·Cu(I)] = 0.100 mmol dm<sup>-3</sup>, [monosaccharide] = 0–7.50 mmol dm<sup>-3</sup> ([D-galactose] = 0–1.50 mmol dm<sup>-3</sup> [D-mannose] = 0–3.00 mmol dm<sup>-3</sup>), MeOH–MeCN = 1 : 1 (v/v), 25 °C.

present system, it is not yet clear which form of furanose *vs.* pyranose is immobilised by the **1a**<sub>2</sub>·Cu(I) complex.<sup>21,24,35</sup> We thus energy-minimised the structure of the ternary **1a**<sub>2</sub>·Cu(I):D-glucose complex using the ESFF forcefield with molecular mechanics (see Experimental section) assuming both the furanose form and the pyranose form for the D-glucose moiety.<sup>36</sup> For the **1a**<sub>2</sub>·Cu(I):D-glucopyranose complex, there was no significant difference between the P-isomer and the M-isomer. On the other hand, the energy-minimised structure for the P-isomer of **1a**<sub>2</sub>·Cu(I):D-glucopyranose is more or less symmetrical whereas that for the M-isomer is sterically distorted (Fig. 9). Careful examination of the D-glucopyranose moiety reveals that (i) in the Newman projection of the 1C–2C bond, the P-isomer can adopt an energetically-favourable staggered conformation whereas the M-isomer is enforced to adopt an energetically-unfavourable eclipsed conformation and (ii) the pyranose ring in the P-isomer is a chair form whereas that in the M-isomer is a twisted boat form. These lines of conformational difference should be effective to stabilise the P-isomer in preference to the M-isomer.

#### On the 'optical purity' of the **1b**<sub>2</sub>·Cu(I)-D-glucose complex

The **1a**<sub>2</sub>·Cu(I) complex is an interconvertible racemic mixture of the P- and M-isomer. The complexation with the D-saccharide results in a diastereomeric mixture of **1a**<sub>2</sub>·Cu(I)-D-saccharide. Since the P:M ratio is changed by the D-saccharide binding, we tried to estimate the 'optical purity' of the P- or M-isomer induced by the binding of the D-saccharide. It seemed to us that

**Fig. 9** Energy-minimised structures for the P-isomer and the M-isomer for **1a**<sub>2</sub>·Cu(I)-D-glucopyranose.

<sup>1</sup>H NMR spectroscopy is the sole tool able to solve this problem. To obtain clear <sup>1</sup>H NMR spectra we chose D-glucose, as this gave the largest  $K_b$  value.<sup>37</sup> As shown in the CD spectral measurements, the reaction rate for D-glucose binding is fairly slow. We therefore left the samples for 6 h at room temperature and then started the <sup>1</sup>H NMR measurements.

Basically, the **1a**<sub>2</sub>·Cu(I)-D-glucose complex involves two chiral centers, one in the (phenanthroline)<sub>2</sub>·Cu(I) moiety (P *versus* M) and the other in the bound D-glucose moiety. As a result, it provides a diastereomeric mixture, which should give the split <sup>1</sup>H NMR peaks. In the <sup>1</sup>H NMR spectrum of the **1a**<sub>2</sub>·Cu(I)-D-glucose complex, however, we could find no such sharp peak that would be conveniently useful as a marker for peak splitting. We thus synthesised **1b**, expecting that the *p*-anisyl group would be useful as a marker. Compound **1b** showed complexation properties (as in Figs. 1 and 2) similar to **1a** and the **1b**<sub>2</sub>·Cu(I) complex showed binding properties for D-glucose (as in Figs. 3, 4 and 5) similar to the **1a**<sub>2</sub>·Cu(I) complex. The 1 : 1 stoichiometry between **1b**<sub>2</sub>·Cu(I) and D-glucose was corroborated not only by a Job plot (as in Fig. 5) but also by ESI-MS spectrometry ( $m/z = 1250$ , which is assignable to

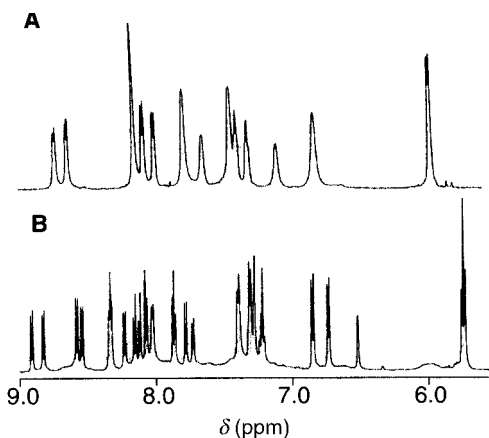


**Fig. 10**  $^1\text{H}$  NMR spectra [600 MHz,  $\text{CD}_3\text{CN}-\text{CD}_3\text{OD} = 1:1$  (v/v)] of  $\mathbf{1b}_2\cdot\text{Cu}(\text{i})$  ( $5.00 \times 10^{-3}$  mol  $\text{dm}^{-3}$ ) at  $-15^\circ\text{C}$  in the absence (A) and the presence (B) of D-glucose ( $12.5 \times 10^{-3}$  mol  $\text{dm}^{-3}$ ).

$[\mathbf{1b}_2\cdot\text{Cu}(\text{i})\cdot\text{D-glucose}]^+$ ). From plots of the CD intensity at 322 nm and 459 nm vs. [D-glucose] the  $K_b$  was estimated to be  $3900 \pm 200$   $\text{dm}^3 \text{mol}^{-1}$ .

As shown in Fig. 10, the *ortho*-protons in the anisole moieties appeared as a doublet peak due to the coupling with the *meta*-protons in the absence of D-glucose. In the presence of D-glucose it changed into a pair of doublets. This change can be explained in two different ways: that is, (i) as mentioned above, the racemic mixture of  $\mathbf{1b}_2\cdot\text{Cu}(\text{i})$  becomes a diastereomeric mixture after binding of D-glucose (Rationale A) or (ii) binding of D-glucose changes the interconvertible racemic mixture into the P-isomer of  $\mathbf{1b}_2\cdot\text{Cu}(\text{i})\cdot\text{D-glucose}$  and the two anisole moieties become inequivalent because of the unsymmetrical structure induced by the bound D-glucose (Rationale B). We believe that this splitting pattern should be attributed to Rationale B because (i) strong CD spectra were observed for both  $\mathbf{1a}_2\cdot\text{Cu}(\text{i})\cdot\text{D-glucose}$  and  $\mathbf{1b}_2\cdot\text{Cu}(\text{i})\cdot\text{D-glucose}$ , the  $\theta$  values ( $1.03 \times 10^4$   $\text{deg cm}^2 \text{dmol}^{-1}$  at 464 nm and  $1.06 \times 10^4$   $\text{deg cm}^2 \text{dmol}^{-1}$  at 459 nm, respectively) of which are comparable with those of optically-pure, bipyridine-based helicate-Cu(i) complexes (*ca.*  $1.5 \times 10^4$   $\text{deg cm}^2 \text{dmol}^{-1}$  at 450–475 nm,<sup>6</sup>  $1.73 \times 10^4$   $\text{deg cm}^2 \text{dmol}^{-1}$  at 479.3 nm<sup>9</sup>), (ii) large  $[\alpha]_D^{25}$  values were observed for  $\mathbf{1a}_2\cdot\text{Cu}(\text{i})\cdot\text{D-glucose}$  and  $\mathbf{1b}_2\cdot\text{Cu}(\text{i})\cdot\text{D-glucose}$  [ $+2520$  and  $+1300^\circ$ , respectively:  $c = 0.048$  g/100 ml ( $\mathbf{1a}_2\cdot\text{Cu}(\text{i})\cdot\text{D-glucose}$ ),  $0.062$  g/100 ml ( $\mathbf{1b}_2\cdot\text{Cu}(\text{i})\cdot\text{D-glucose}$ ), solvent: MeCN–MeOH = 1:1 (v/v)], which are sufficiently greater than those of optically-pure, bipyridine-based helicate-Cu(i) complex ( $+361$ ,<sup>6</sup>  $+501$ <sup>9</sup>) and (iii) the absorption spectral change which reflects the binding of D-glucose to  $\mathbf{1a}_2\cdot\text{Cu}(\text{i})$  or  $\mathbf{1b}_2\cdot\text{Cu}(\text{i})$  was completed in a few minutes after the D-glucose addition<sup>38</sup> whereas the CD spectral change which reflects the P–M isomerisation took several hours. Points (i) and (ii) clearly rule out the possibility that  $\mathbf{1b}_2\cdot\text{Cu}(\text{i})\cdot\text{D-glucose}$  is a diastereomeric mixture. Point (iii) is observable only when the P–M isomerisation proceeds within the  $\mathbf{1a}_2\cdot\text{Cu}(\text{i})\cdot\text{D-glucose}$  and  $\mathbf{1b}_2\cdot\text{Cu}(\text{i})\cdot\text{D-glucose}$  complexes. These lines of evidence clearly support the view that the  $\mathbf{1b}_2\cdot\text{Cu}(\text{i})\cdot\text{D-glucose}$  complex is not the diastereomeric mixture (Rationale A) but the P-isomer with the high optical purity. Judging from the sensitivity of the present 600 MHz  $^1\text{H}$  NMR apparatus, 5% of the isomer should be easily detectable (if it exists). We thus believe that the optical purity is higher than 95%.

## Experimental

### Materials

2-Phenyl-9-*p*-tolyl-1,10-phenanthroline (**2a**) and 2-anisyl-9-*p*-tolyl-1,10-phenanthroline (**2b**) were prepared according to the

method of Goodman *et al.*<sup>3</sup> and identified by IR and  $^1\text{H}$  NMR spectral evidence and elemental analysis.

**2-(*p*-Methylaminomethylphenyl)-9-phenyl-1,10-phenanthroline (4a).** Compound **2a** (2.22 g, 6.4 mmol) was treated with *N*-bromosuccinimide (NBS) (1.37 g, 7.7 mmol) and  $\alpha,\alpha'$ -azobisisobutyronitrile (0.14 g, 10 wt% of NBS) in  $\text{CCl}_4$  at the reflux temperature for 50 min. The progress of the reaction was followed by  $^1\text{H}$  NMR spectroscopy [250 MHz,  $\text{CCl}_4\text{-CDCl}_3 = 1:1$  (v/v)] with the disappearance of  $\delta_{\text{CH}_3}$ , 2.47 ppm and the appearance of  $\delta_{\text{CH}_2\text{Br}}$ , 4.60 ppm. After cooling, the insoluble materials were removed by filtration, the filtrate being dried over  $\text{Na}_2\text{SO}_4$ . This solution containing **3a** was used for the synthesis of **4a** without further purification. Into the  $\text{CCl}_4$  solution cooled with an ice-bath was introduced methylamine gas for 4 h. The progress of the reaction was followed by a TLC method [silica gel,  $\text{CH}_2\text{Cl}_2\text{-MeOH} = 10:1$  (v/v)]. After 4 h when the spot for **3a** ( $R_f = 0.90$ ) disappeared, the reaction was finished by the addition of aqueous 5%  $\text{NaHCO}_3$  solution. The mixture was stirred for one day and then the insoluble materials were removed by filtration. The  $\text{CCl}_4$  layer was washed three times with aqueous 5%  $\text{NaHCO}_3$  solution and then dried over  $\text{Na}_2\text{SO}_4$ . The solution was concentrated to dryness, the solid residue being further purified through chromatography [silica gel, column  $\phi$  2.5  $\times$  17 cm,  $\text{CH}_2\text{Cl}_2\text{-MeOH} = 10:1$  (v/v)] to yield **4a**, 1.55 g (62%, calculated from **2a**), slightly yellow powder, mp  $83\text{--}87^\circ\text{C}$ ;  $^1\text{H}$  NMR ( $\text{CDCl}_3$ , 600 MHz,  $27^\circ\text{C}$ )  $\delta$  2.60 (3H, s, NH- $\text{CH}_3$ ), 4.04 (2H, s, Ar- $\text{CH}_2\text{-NH}$ ), 7.52 (1H, t (7.2 Hz), 9-phenyl- $H_p$ ), 7.60 (2H, d (7.6 Hz), 2-phenyl- $H_m$ ), 7.61 (2H, t (7.6 Hz), 9-phenyl- $H_m$ ), 7.70, 7.74 (2H, d  $\times$  2 (8.6 Hz), phen- $H_{5,6}$ ), 7.98 (1H, d (8.3 Hz), phen- $H_3$ ), 8.11 (1H, d (8.3 Hz), phen- $H_8$ ), 8.23 (3H, d (7.9 Hz), phen- $H_4$ , 2-phenyl- $H_o$ ), 8.29 (1H, d (8.3 Hz), phen- $H_7$ ), 8.36 (2H, d (7.6 Hz), 9-phenyl- $H_o$ ); Anal. Calcd. for  $\text{C}_{26}\text{H}_{21}\text{N}_3$ : C, 83.18; H, 5.64; N, 11.19%. Found: C, 83.14; H, 6.06; N, 11.20%.

**1-{*N*-Methyl-*N*-[2-(dihydroxyboryl)phenylmethyl]amino-methyl}-4-(9-phenyl-1,10-phenanthrolin-2-yl)benzene (1a).** Compound **4a** (1.30 g, 3.5 mmol) and 2-(2-bromomethylphenyl)-1,3-dioxaborinane (1.15 g, 4.5 mmol) were treated in refluxing acetonitrile (100 ml) in the presence of  $\text{K}_2\text{CO}_3$  (0.96 g, 6.9 mmol). The progress of the reaction was followed by a TLC method [silica gel,  $\text{CH}_2\text{Cl}_2\text{-MeOH} = 5:1$  (v/v)]. After 17 h when the spot for **1a** ( $R_f = 0.45$ ) disappeared, the reaction was finished. After cooling, the insoluble materials were filtered off, the filtrate being evaporated to dryness. The solid residue was taken with a mixture of dichloromethane and aqueous 5%  $\text{NaHCO}_3$  solution and the phase-separated mixture was stirred for 30 min. The organic layer was separated, washed with water and dried over  $\text{Na}_2\text{SO}_4$ . The solution was concentrated to dryness, the solid residue being further purified through chromatography [silica gel, column  $\phi$  2.5  $\times$  15 cm,  $\text{CH}_2\text{Cl}_2\text{-MeOH} = 5:1$  (v/v)] to yield **1a**, 0.93 g (46%), slightly yellow powder, mp  $174\text{--}179^\circ\text{C}$ ; IR (KBr)  $\nu_{\text{B-O}}$   $1340 \text{ cm}^{-1}$ ;  $^1\text{H}$  NMR (600 MHz,  $\text{CDCl}_3$ ,  $27^\circ\text{C}$ )  $\delta$  2.19 (3H, s, N- $\text{CH}_3$ ), 3.80, 3.83 (4H, s  $\times$  2, - $\text{CH}_2\text{-NMe-CH}_2\text{-}$ ), 7.25 (1H, d (6.7 Hz), borylphenyl- $H_6$ ), 7.38 (2H, t (7.1 Hz), borylphenyl- $H_{4,5}$ ), 7.50 (1H, t (8.2 Hz), 9-phenyl- $H_p$ ), 7.51 (2H, t (8.1 Hz), benzene- $H_2$ ), 7.60 (2H, t (7.6 Hz), 9-phenyl- $H_m$ ), 7.80 (2H, s, phen- $H_{5,6}$ ), 7.97 (1H, d (6.7 Hz), borylphenyl- $H_3$ ), 8.13, 8.15 (2H, d  $\times$  2 (8.4 Hz), phen- $H_{3,8}$ ), 8.32 (2H, d (8.3 Hz), 9-phenyl- $H_o$ ), 8.46 (4H, m, phen- $H_{4,7}$ , benzene- $H_3$ ); Anal. Calcd. for  $\text{C}_{33}\text{H}_{26}\text{N}_3\text{BO} + 0.3\text{H}_2\text{O}$ : C, 79.91; H, 5.50; N, 8.31%. Found: C, 79.79; H, 5.40; N, 8.46%.

**2-(*p*-Methylaminomethylphenyl)-9-*p*-anisyl-1,10-phenanthroline (4b).** Compound **2b** (4.11 g, 10.9 mmol) was treated with *N*-bromosuccinimide (NBS) (2.33 g, 13.1 mmol) and  $\alpha,\alpha'$ -azobisisobutyronitrile (0.23 g, 10 wt% of NBS) in  $\text{CCl}_4$  at the reflux temperature for 40 min. The progress of the reaction was followed by  $^1\text{H}$  NMR spectroscopy [250 MHz,  $\text{CCl}_4\text{-CDCl}_3 =$

1:1 (v/v)] with the disappearance of  $\delta_{\text{CH}}$ , 2.47 ppm and the appearance of  $\delta_{\text{CH,Br}}$  4.59 ppm. After cooling, the insoluble materials were removed by filtration, the filtrate being dried over  $\text{Na}_2\text{SO}_4$ . This solution containing **3b** was used for the synthesis of **4b** without further purification. Into the  $\text{CCl}_4$  solution cooled with an ice-bath was introduced methylamine gas for 6 h. The progress of the reaction was followed by a TLC method [silica gel, toluene–MeOH = 10:1 (v/v)]. After 4 h when the spot for **3b** ( $R_f$  = 0.67) disappeared, the reaction was finished by the addition of aqueous 5%  $\text{NaHCO}_3$  solution. The mixture was stirred for one day and then the insoluble materials were removed by filtration. The  $\text{CCl}_4$  layer was washed three times with aqueous 5%  $\text{NaHCO}_3$  solution and then dried over  $\text{Na}_2\text{SO}_4$ . The solution was concentrated to dryness, the solid residue being further purified through chromatography [silica gel, column  $\phi$  5 × 8 cm,  $\text{CHCl}_3$ –MeOH = 5:1 (v/v)] to yield **4b**, 1.99 g (46%, calculated from **2b**), slightly yellow powder, mp 42–48 °C;  $^1\text{H NMR}$  ( $\text{CDCl}_3$ , 250 MHz, 27 °C)  $\delta$  2.51 (3H, s, NH- $\text{CH}_3$ ), 3.87 (2H, s, Ar- $\text{CH}_2$ -NH), 3.92 (3H, s, - $\text{OCH}_3$ ), 7.11 (2H, d (8.8 Hz), 2-phenyl- $H_m$ ), 7.41 (2H, d (8.1 Hz), 9-phenyl- $H_m$ ), 7.76 (2H, s, phen- $H_{5,6}$ ), 8.09 (1H, d (8.5 Hz), phen- $H_3$ ), 8.13 (1H, d (9.8 Hz), phen- $H_8$ ), 8.26 (1H, d (7.2 Hz), phen- $H_4$ ), 8.29 (1H, d (8.3 Hz), phen- $H_7$ ), 8.44 (4H, d (7.6 Hz), 2-phenyl- $H_m$ , 9-phenyl- $H_o$ ); Anal. Calcd. for  $\text{C}_{27}\text{H}_{23}\text{N}_3\text{O} + 0.4\text{H}_2\text{O}$ : C, 78.57; H, 5.81; N, 10.18%. Found: C, 78.65; H, 5.70; N, 10.09%.

**1-{N-Methyl-N-[2-(dihydroxyboryl)phenylmethyl]amino-methyl}-4-(9-p-anisyl-1,10-phenanthrolin-2-yl)benzene (1b)**  
Compound **4b** (1.80 g, 4.4 mmol) and 2-(2-bromomethyl-phenyl)-1,3-dioxaborinane (1.47 g, 5.8 mmol) were treated in refluxing acetonitrile (100 ml) in the presence of  $\text{K}_2\text{CO}_3$  (1.23 g, 8.9 mmol). The progress of the reaction was followed by a TLC method [silica gel,  $\text{CHCl}_3$ –MeOH = 5:1 (v/v)]. After 6 h when the spot for **4b** ( $R_f$  = 0.13) disappeared, the reaction was finished. After cooling, the insoluble materials were filtered off, the filtrate being evaporated to dryness. The solid residue was taken with a mixture of dichloromethane and aqueous 5%  $\text{NaHCO}_3$  solution and the phase-separated mixture was stirred for 30 min. The organic layer was separated, washed with water and dried over  $\text{Na}_2\text{SO}_4$ . The solution was concentrated to dryness, the solid residue being further purified through chromatography [silica gel, column  $\phi$  5 × 10 cm,  $\text{CHCl}_3$ –MeOH = 5:1 (v/v)] to yield **1b**, 0.81 g (34%), slightly yellow powder, mp 178–183 °C; IR (KBr)  $\nu_{\text{B-O}}$  1344  $\text{cm}^{-1}$ ;  $^1\text{H NMR}$  (600 MHz,  $\text{CDCl}_3$ , 27 °C)  $\delta$  2.20 (3H, s, N- $\text{CH}_3$ ), 3.69, 3.79 (4H, s × 2, - $\text{CH}_2$ -NMe- $\text{CH}_2$ -), 3.93 (3H, s, - $\text{OCH}_3$ ), 7.13 (2H, d (8.5), 9-phenyl- $H_m$ ), 7.25 (1H, d (6.9 Hz), borylphenyl- $H_6$ ), 7.38 (2H, t (7.1 Hz), borylphenyl- $H_{4,5}$ ), 7.51 (2H, d (8.0 Hz), benzene- $H_2$ ), 7.77 (2H, d × 2 (8.9 Hz), phen- $H_{5,6}$ ), 7.97 (1H, d (6.4 Hz), borylphenyl- $H_3$ ), 8.10, 8.12 (2H, d × 2 (8.4 Hz), phen- $H_{3,8}$ ), 8.27 (2H, d (8.4 Hz), phen- $H_{4,7}$ ), 8.43 (4H, d (8.0 Hz), phen- $H_{4,7}$ , 9-phenyl- $H_o$ , benzene- $H_3$ ); Anal. Calcd. for  $\text{C}_{34}\text{H}_{30}\text{N}_3\text{BO}_2 + 0.5\text{H}_2\text{O}$ : C, 76.98; H, 5.51; N, 7.92%. Found: C, 77.12; H, 5.36; N, 7.94%.

#### Miscellaneous

$^1\text{H NMR}$ , absorption spectra, optical rotation, ESI-MS spectra and CD spectra were measured with Bruker DMX 600, JASCO V-570, HORIBA SEPA-300, Perseptive Mariner and JASCO J-720 WI, respectively. The energy minimisation of the **1a** $\cdot$ Cu(I) $\cdot$ D-glucose complexes was performed using the ESFF forcefield with molecular mechanics as implemented by Discover (MSI).

#### Acknowledgements

This work was supported by a Grant-in-Aid for COE Research 'Design and Control of Advanced Molecular Assembly

Systems' from the Ministry of Education, Science and Culture, Japan (#08CE2005).

#### References

- For a recent comprehensive review see: E. C. Constable, in *Comprehensive Supramolecular Chemistry*, ed. J.-M. Lehn, Pergamon, Oxford, 1996, vol. 9, p. 213; A. F. Williams, *Chem. Eur. J.*, 1997, **3**, 15; C. Piguet, G. Bernardinelli and G. Hopfgartner, *Chem. Rev.*, 1997, **97**, 2005; A. E. Rowan and R. J. M. Nolte, *Angew. Chem., Int. Ed. Engl.*, 1998, **37**, 63.
- C. J. Carrano and K. N. Raymond, *J. Am. Chem. Soc.*, 1978, **100**, 5371; B. Kersting, M. Meyer, R. E. Powers and K. N. Raymond, *J. Am. Chem. Soc.*, 1996, **118**, 7221.
- J. Libman, Y. Tor and A. Shnitzer, *J. Am. Chem. Soc.*, 1987, **109**, 5880; L. Zelikovich, J. Libman and A. Shnitzer, *Nature*, 1995, **374**, 790; C. Bianchini, A. Meli, V. Patinec, V. Sernau and F. Vizza, *J. Am. Chem. Soc.*, 1997, **119**, 4945.
- S. Christie, I. F. Fraser, A. McVitie and R. D. Peacock, *Polyhedron*, 1986, **5**, 35; P. Agaskar, F. A. Cotton, I. F. Fraser and R. D. Peacock, *J. Am. Chem. Soc.*, 1984, **106**, 1851; P. A. Agaskar, F. A. Cotton, I. F. Fraser, L. Manojlovic-Muir, K. W. Muir and R. D. Peacock, *Inorg. Chem.*, 1986, **25**, 2511.
- M. Gerards, *Inorg. Chim. Acta*, 1995, **229**, 101.
- W. Zarges, J. Hall and J.-M. Lehn, *Helv. Chim. Acta*, 1991, **74**, 1843.
- E. C. Constable, T. Kulke, M. Neuburger, M. Zehnder, *Chem. Commun.*, 1997, 489; G. Baum, E. C. Constable, D. Fenske and T. Kulke, *Chem. Commun.*, 1997, 2043; G. Baum, E. C. Constable, D. Fenske, C. E. Housecroft and T. Kulke, *Chem. Commun.*, 1998, 2659.
- C. Provent, S. Hewage, G. Brand, G. Bernardinelli, L. J. Charbonniere and A. F. Williams, *Angew. Chem., Int. Ed. Engl.*, 1997, **36**, 1287.
- C. R. Woods, M. Benaglia, F. Cozzi and J. S. Siegel, *Angew. Chem., Int. Ed. Engl.*, 1996, **35**, 1830; C. R. Woods, M. Benaglia, P. Blom, A. Fuchicello, F. Cozzi and J. S. Siegel, *Polym. Prepr.*, 1996, **37**, 480.
- A. L. Airey, G. F. Swiegers, A. C. Willis and S. B. Wild, *J. Chem. Soc., Chem. Commun.*, 1995, 695.
- T. Suzuki, H. Kotsuki, K. Isobe, N. Moriya, Y. Nakagawa and M. Ochi, *Inorg. Chem.*, 1995, **34**, 530.
- J. F. Modder, G. van Koten, K. Vrieze and A. L. Spek, *Angew. Chem., Int. Ed. Engl.*, 1989, **28**, 1698; J. F. Modder, K. Vrieze, A. L. Spek, G. Challa and G. Van Koten, *Inorg. Chem.*, 1992, **31**, 1238.
- Y. Dai, T. J. Katz and D. A. Nichols, *Angew. Chem., Int. Ed. Engl.*, 1996, **35**, 2109.
- E. J. Enemark and T. D. P. Stack, *Angew. Chem., Int. Ed. Engl.*, 1995, **34**, 996.
- M. Albrecht, *Synlett.*, 1996, 565.
- M. S. Goodman, A. D. Hamilton and J. Weiss, *J. Am. Chem. Soc.*, 1995, **117**, 8447.
- J. Yoon and A. W. Czarnik, *J. Am. Chem. Soc.*, 1992, **114**, 5874; L. K. Mohler and A. W. Czarnik, *ibid.*, 1993, **115**, 2998.
- P. R. Westmark and B. D. Smith, *J. Am. Chem. Soc.*, 1994, **116**, 9343 and references cited therein.
- Y. Nagai, K. Kobayashi, H. Toi and Y. Aoyama, *Bull. Chem. Soc. Jpn.*, 1993, **66**, 2965.
- G. Wulff, S. Krieger, B. Kubneweg and A. Steigel, *J. Am. Chem. Soc.*, 1994, **116**, 409 and references cited therein.
- J. C. Norrild and H. Eggert, *J. Am. Chem. Soc.*, 1995, **117**, 1479.
- For comprehensive reviews on boronic acid-based saccharide receptors, see: T. D. James, K. R. A. S. Sandanayake and S. Shinkai, *Supramol. Chem.*, 1995, **6**, 141; T. D. James, P. Linnane and S. Shinkai, *Chem. Commun.*, 1996, 281; T. D. James, K. R. A. S. Sandanayake and S. Shinkai, *Angew. Chem., Int. Ed. Engl.*, 1996, **35**, 1911; K. R. A. S. Sandanayake, T. D. James and S. Shinkai, *Pure Appl. Chem.*, 1996, **68**, 1207; S. Shinkai and M. Takeuchi, *Trends Anal. Chem.*, 1996, **15**, 188.
- K. Tsukagoshi and S. Shinkai, *J. Org. Chem.*, 1991, **56**, 4089; Y. Shiomi, M. Saisho, K. Tsukagoshi and S. Shinkai, *J. Chem. Soc., Perkin Trans. 1*, 1993, 2111.
- T. D. James, K. R. A. S. Sandanayake and S. Shinkai, *Angew. Chem.*, 1994, **106**, 2287; T. D. James, K. R. A. S. Sandanayake and S. Shinkai, *Angew. Chem., Int. Ed. Engl.*, 1994, **22**, 2207; T. D. James, K. R. A. S. Sandanayake and S. Shinkai, *J. Chem. Soc., Chem. Commun.*, 1994, 477.
- M. Takeuchi, T. Imada and S. Shinkai, *J. Am. Chem. Soc.*, 1996, **118**, 10658; M. Takeuchi, T. Imada and S. Shinkai, *Bull. Chem. Soc. Jpn.*, 1998, **71**, 1117; M. Takeuchi, T. Mizuno, H. Shinmori, M. Nakashima and S. Shinkai, *Tetrahedron*, 1996, **52**, 1195; M. Takeuchi, S. Yoda, T. Imada and S. Shinkai, *Tetrahedron*, 1997,

- 53, 8335; H. Shinmori, M. Takeuchi and S. Shinkai, *J. Chem. Soc., Perkin Trans. 2*, 1998, 847.
- 26 T. Imada, H. Kijima, M. Takeuchi and S. Shinkai, *Tetrahedron*, 1996, **52**, 2817; M. Yamamoto, M. Takeuchi and S. Shinkai, *Tetrahedron*, 1998, **54**, 3125; M. Takeuchi, M. Taguchi, H. Shinmori and S. Shinkai, *Bull. Chem. Soc. Jpn.*, 1996, **69**, 2613.
- 27 S. Arimori, M. Takeuchi and S. Shinkai, *J. Am. Chem. Soc.*, 1996, **118**, 245; T. Kimura and S. Shinkai, *Chem. Lett.*, 1998, 1035; T. Kimura, M. Takeuchi and S. Shinkai, *Bull. Chem. Soc. Jpn.*, 1998, **71**, 2197.
- 28 M. Mikami and S. Shinkai, *J. Chem. Soc., Chem. Commun.*, 1995, 153; M. Mikami and S. Shinkai, *Chem. Lett.*, 1995, 603; M. Takeuchi, Y. Chin, T. Imada and S. Shinkai, *Chem. Commun.*, 1996, 1867.
- 29 T. Mizuno, M. Takeuchi, I. Hamachi, K. Nakashima and S. Shinkai, *J. Chem. Soc., Perkin Trans. 2*, 1998, 2281; G. Nuding, K. Nakashima, R. Iguchi, T. Ishi-i and S. Shinkai, *Tetrahedron Lett.*, 1998, **39**, 9473.
- 30 M. Takeuchi, K. Koumoto, M. Goto and S. Shinkai, *Tetrahedron*, 1996, **52**, 12931.
- 31 Preliminary communication: M. Yamamoto, M. Takeuchi and S. Shinkai, *Tetrahedron Lett.*, 1998, **39**, 1189.
- 32 J. A. Nelder and R. Mead, *Comput. J.*, 1965, **7**, 308; S. L. Morgan and S. N. Deming, *Anal. Chem.*, 1974, **46**, 1170.
- 33 T. D. James, K. R. A. S. Sandanayake, R. Iguchi and S. Shinkai, *J. Am. Chem. Soc.*, 1995, **117**, 8982; T. D. James, K. R. A. S. Sandanayake and S. Shinkai, *Nature*, 1995, **374**, 345.
- 34 K. Kondo, Y. Shiomi, M. Saisho, T. Harada and S. Shinkai, *Tetrahedron*, 1992, **48**, 8239; T. D. James and S. Shinkai, *Chem. Commun.*, 1995, 1483.
- 35 M. Bielecki, H. Eggert and J. C. Norrild, *J. Chem. Soc., Perkin Trans. 2*, 1999, 449.
- 36 Here, we take only the  $\alpha$ -anomer into consideration, because it has a 1,2-*cis*-diol group that can bind a boronic acid group by forming a cyclic ester, whereas the  $\beta$ -anomer, having a 1,2-*trans* diol group, cannot or finds it very difficult to form such a cyclic ester.
- 37 To simplify the  $^1\text{H}$  NMR spectral pattern  $C_2$ -symmetrical saccharides such as D-threitol and D-mannitol-3,4-carbonate would be more suitable for the present system than  $C_2$ -unsymmetrical D-glucose. Unfortunately, the affinity of these  $C_2$ -symmetrical saccharides with the  $\mathbf{1a}_2\cdot\text{Cu(I)}$  complex was not as high and the resultant  $^1\text{H}$  NMR spectra were very complex because of overlap with uncomplexed saccharides.
- 38 The concentrations used for the  $^1\text{H}$  NMR measurements ( $[\mathbf{1b}_2\cdot\text{Cu(I)}] = 5.00 \text{ mmol dm}^{-3}$  and  $[\text{D-glucose}] = 12.5 \text{ mmol dm}^{-3}$  in Fig. 10) are much higher than those used for the CD measurements ( $[\mathbf{1a}_2\cdot\text{Cu(I)}] = [\text{D-glucose}] = 0.100 \text{ mmol dm}^{-3}$  in Fig. 3). This is why the equilibrium is attained much faster in  $^1\text{H}$  NMR measurements than in the CD measurements.

Paper a904936c